AIAA Propulsion and Energy Forum
19-22 August 2019, Indianapolis, IN
AIAA Propulsion and Energy 2019 Forum

10.2514/6.2019-4223

Characterization of spray structures formed during water injection into a free supersonic air jet

Shyam Menon*, Hansen Jones†, James Leung‡, Wei Zhao§

Louisiana State University, Baton Rouge, LA, 70803

The interaction of a water jet with a free supersonic air jet results in the formation of a spray with characteristics different from a traditional jet in crossflow. The unbounded nature of the free supersonic jet and the presence of Mach diamonds in the flow contribute to the differences observed in the spray structure formed during the interaction of the two jets. This work utilizes non-intrusive diagnostics to study the interaction process and the resulting flow field. The spray generated by the interaction of a supersonic free air jet with water jet issued from three types of nozzles is studied. The nozzles include one that produces a coherent water jet, another that produces a fan-spray and a third that generates a full-cone spray. Diffused back-lit imaging using a laser light source and synchronized high-speed imaging is used to obtain frozen images of the spray. Volume illuminated high-speed imaging is used to track the spray penetration into the air jet. The measurements highlight unique features of the spray formation process and differences between the current observations and structures found in traditional jet-in-crossflow interactions are analyzed.

I. Introduction

The interaction of a coherent liquid jet with a free supersonic jet is of relevance to several engineering applications including noise reduction in aircraft jet exhaust [1] as well as cooling of hot exhaust during rocket test applications [2]. The interaction process is significantly different from a traditional bounded, supersonic, jet-in-crossflow (JICF) due to several key reasons. **Figure 1** shows schematically the differences in the two configurations, with bounded JICF shown on the left and liquid jet injection into a free supersonic gas jet on the right.

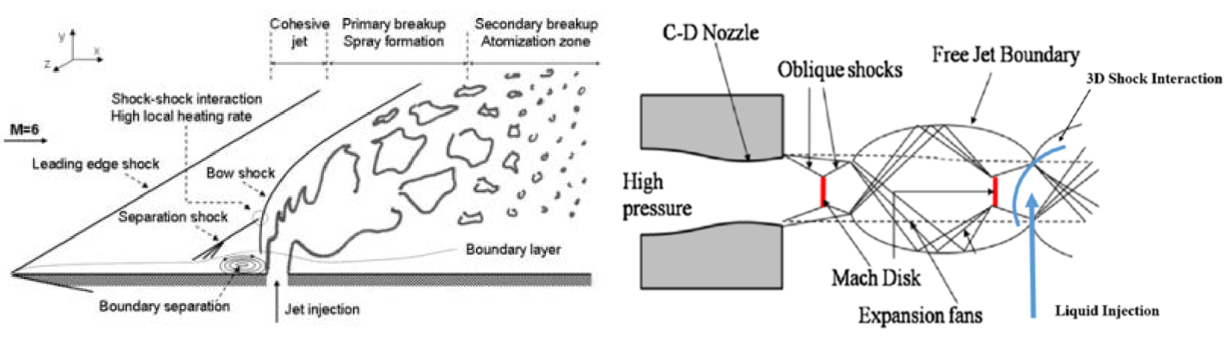

Figure 1. Left: Jet in crossflow [3], Right: Liquid penetration in a free jet – Adapted from [4].

Since the jet in crossflow is traditionally studied as it relates to fuel injection into supersonic combustion chambers, the upstream gas flow is generally uniform and contains no internal shockwave structure. For the injection configuration of interest in this work, the gas phase is expanded to a pressure less than ambient prior to injection into the ambient atmosphere, resulting in an over-expanded flow with an inherent internal

* Assistant Professor, Mechanical and Industrial Engineering Department, smenon@lsu.edu
† Graduate Research Assistant, Mechanical and Industrial Engineering Department, hansen.j.jones@gmail.com
‡ Graduate Research Assistant, Mechanical and Industrial Engineering Department, jleung3@lsu.edu
§ Undergraduate Researcher, Mechanical and Industrial Engineering Department, weizhao3452@gmail.com

shockwave structure. Additionally, the bounded nature of the traditional jet in crossflow allows the liquid flow to be influenced by the gas phase flow continuously while the free jet configuration is inherently three-dimensional in nature, allowing the liquid phase to be displaced outside of the gas flow or even penetrate it completely. This lack of constraint in the case of the free jet as imposed by a solid boundary potentially introduces several changes in the flow structure from that in the bounded JICF. Finally, for the present configuration, the finite sizes of the liquid jet and gas jet results in a different interaction from the traditional bounded JICF, where the liquid views the gas jet as a continuum and is continuously influenced by the crossflow during the interaction process. Investigating these differences to obtain a phenomenological understanding of the interaction and resulting spray formation is a key motivation for this work.

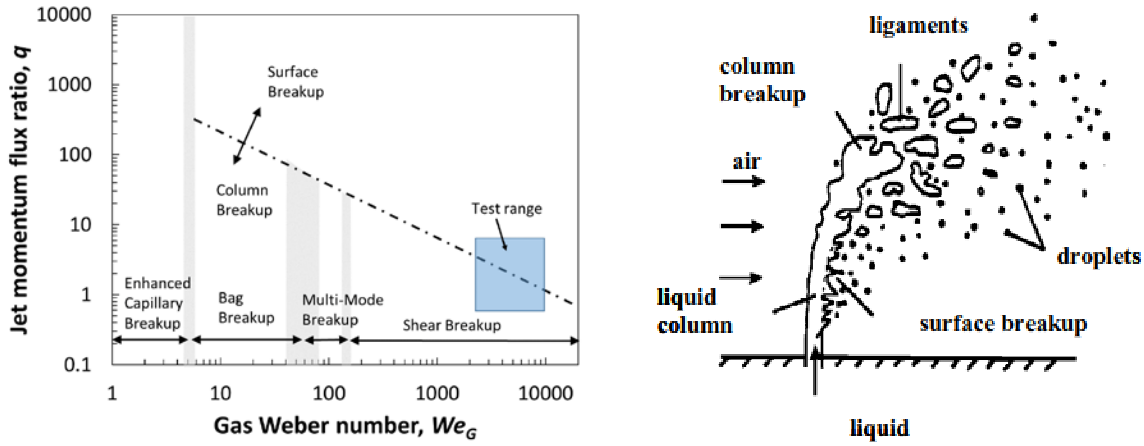

Figure 2: Regime map for spray breakup [5] with location of current test region (Left); Illustration of column and surface breakup [5] (Right).

The results of this investigation are highly pertinent to understanding the water spray-based rocket exhaust cooling processes used at the test stands at NASA Stennis Space Center (SSC). Given the high gas Weber number (*We*) involved in the interaction process during exhaust cooling, it is likely that the spray breakup process could show features different from those illustrated in the regime diagram presented in **Figure 2** (Left). Traditionally, the spray breakup regime diagram is associated with column and surface breakup as illustrated in **Figure 2** (Right). Column breakup is associated with the formation of column waves, which eventually grow and result in spray breakup while surface breakup is associated with mass loss from the jet through shearing action. This work further aims to generate validation data for ongoing efforts at NASA SSC to develop computational routines to model the spray generation process. In particular, data is required to validate models that capture the primary atomization process incorporating compressibility effects. Finally, it is also desired to investigate the qualitative and quantitative differences in spray generation and water penetration as it pertains to the liquid nozzle configuration. While previous efforts in this project [6][7] have focused on a coherent jet interacting with the crossflow, it is desired to investigate nozzles that produce flat or conical sprays interacting with the crossflow. This is particularly useful since it is more similar to the exhaust cooling setups at NASA SSC and is a relatively easier configuration to model given that the spray can be initialized with an initial distribution of liquid droplets.

Given the motivating factors above, this work investigates the interaction process of a free supersonic air jet with both a coherent water jet as well as water sprays. The studies are carried out in a cold-flow experimental test setup using non-intrusive diagnostics including diffused backlit imaging using a pulsed laser as well as high-speed imaging using volume illumination. Images are analyzed to study the spray formation process as well as to identify the penetration height of the water jet into the cross-flowing air jet. Measured penetration heights are compared with empirical formulations from literature to identify potential configuration-dependent deviations.

II. Experiment

The experimental setup used in this work has been developed by Hansen [6], in previous studies related to this effort [7]. The setup shown in **Figure 3** consists of a converging-diverging nozzle that utilizes high-pressure air (up to 150 psig) supplied from a compressor to generate a supersonic air flow. A nozzle supplied with water pressurized by air is mounted on a vertical traverse, which allows for changes in injection location. The injection pressure can be varied by varying the air pressure exerted on the surface of water in the water tank.

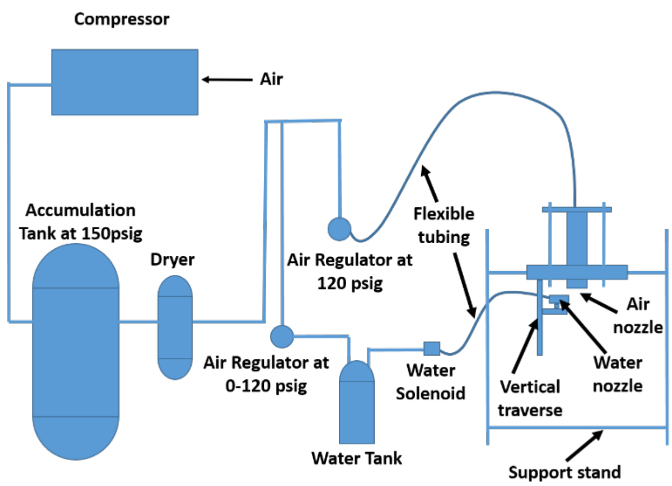

Figure 3: Schematic of experimental setup.

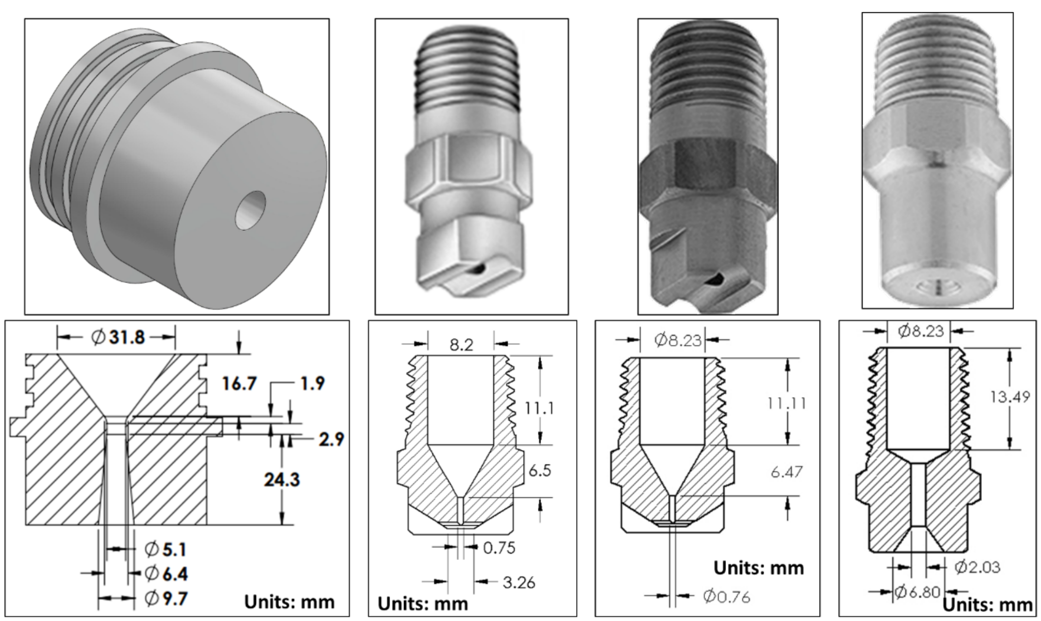

Figure 4: Schematic and dimensions for: C-D nozzle for air; coherent jet water nozzle; fan-spray water nozzle; conical-spray water nozzle.

Three types of nozzles are investigated in this work. ***Table 1*** shows the key specifications of each nozzle. The three types of water nozzles investigated in this work are: nozzle producing a coherent jet;

nozzle producing a full-cone spray; and a nozzle producing a 25^0 angle fan-spray. **Figure 4** shows the geometry of the C-D nozzle used to generate supersonic airflow as well as each of the water spray nozzles. Water injection pressure and injection location are two key parameters that are varied in this work. ***Table 2*** shows a summary of the key operating conditions investigated in this work.

Table 1: Key specifications of the various nozzles tested in this work.

Nozzle #	**Nozzle exit diameter [mm]**	**Nozzle type**
1	1.52	Coherent jet
2	1.02	
3	0.76	
4	0.76	25^0 spray angle fan
5	2.03	Full cone spray

Table 2: Operating parameters for water corresponding to the different injection test cases using the coherent jet nozzles (Nozzles 1, 2, and 3).

Case #	**Water injection pressure [psig]**	**Air injection pressure [psig]**	**Momentum ratio, *q***
1	20	80	0.55
2	30		0.83
3	40		1.11
4	50		1.39
5	60		1.66
6	70		1.94
7	80		2.22
8	90		2.49
9	100		2.77

III. Diagnostics

Two key experimental diagnostics are used in this work. Diffused backlit imaging is used with a high-speed camera to get almost "instantaneous" images of the interaction process. A pulsed laser producing pulses between 3-5 ns long allows the flowfield to be almost frozen in time. The images are taken by a high-speed camera, which is synchronized to the laser pulse. The high-speed camera is a Photron SA-3 model with 1024x1024 pixel resolution at a frame rate of 2,000 fps. In this measurement the laser is operated at 15 Hz and the camera images at 60 fps. **Figure 5** shows photographs of the components used in the diffused backlit imaging as well as a schematic of the setup. A square "engineered" diffuser (Thorlabs ED1-S20-MD) allows for the laser beam to be converted into a square sheet that provides the background to image the spray. The square laser beam is projected on a diffuse background. The high-speed camera is equipped with a 180 mm focal length lens to provide a well-resolved image of the spray formation.

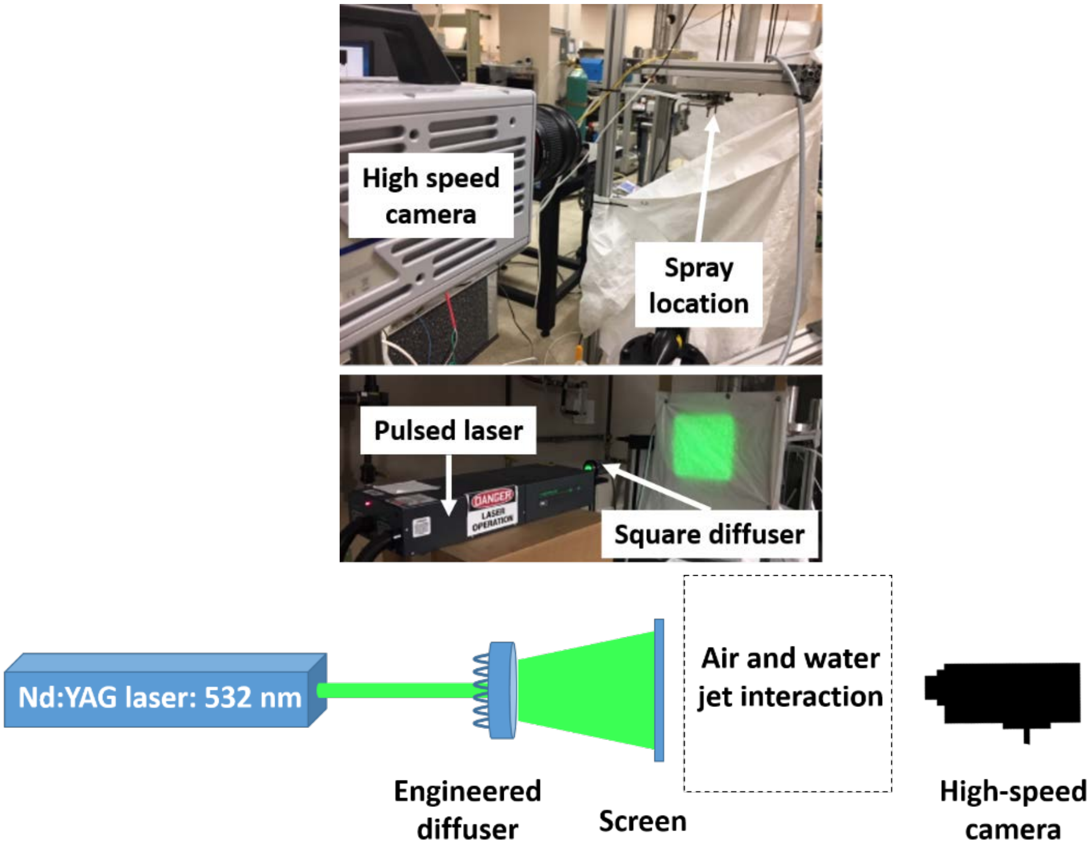

Figure 5: Photographs of the setup used for diffused backlit imaging as well as a schematic.

The high-speed camera is also used with volume illumination in the form of a halogen lamp to obtain longer duration videos (0.5 s). The lamp is placed about 3 meters from the spray setup at an off-angle of 15^0. Images are acquired at 2000 fps. **Figure 6** shows a schematic of the high-speed imaging setup.

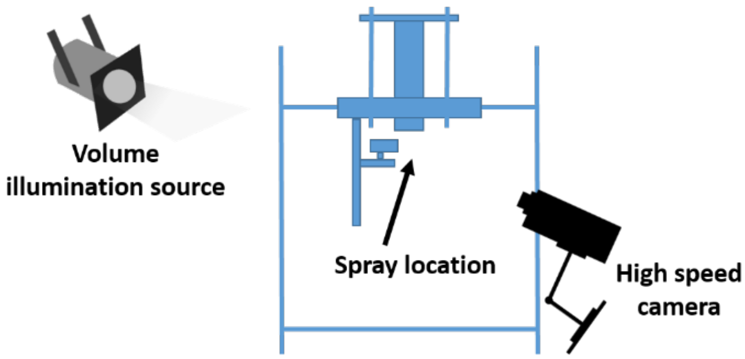

Figure 6: Schematic of the setup used for high-speed imaging with volume illumination.

IV. Results

a. Water jet breakup process

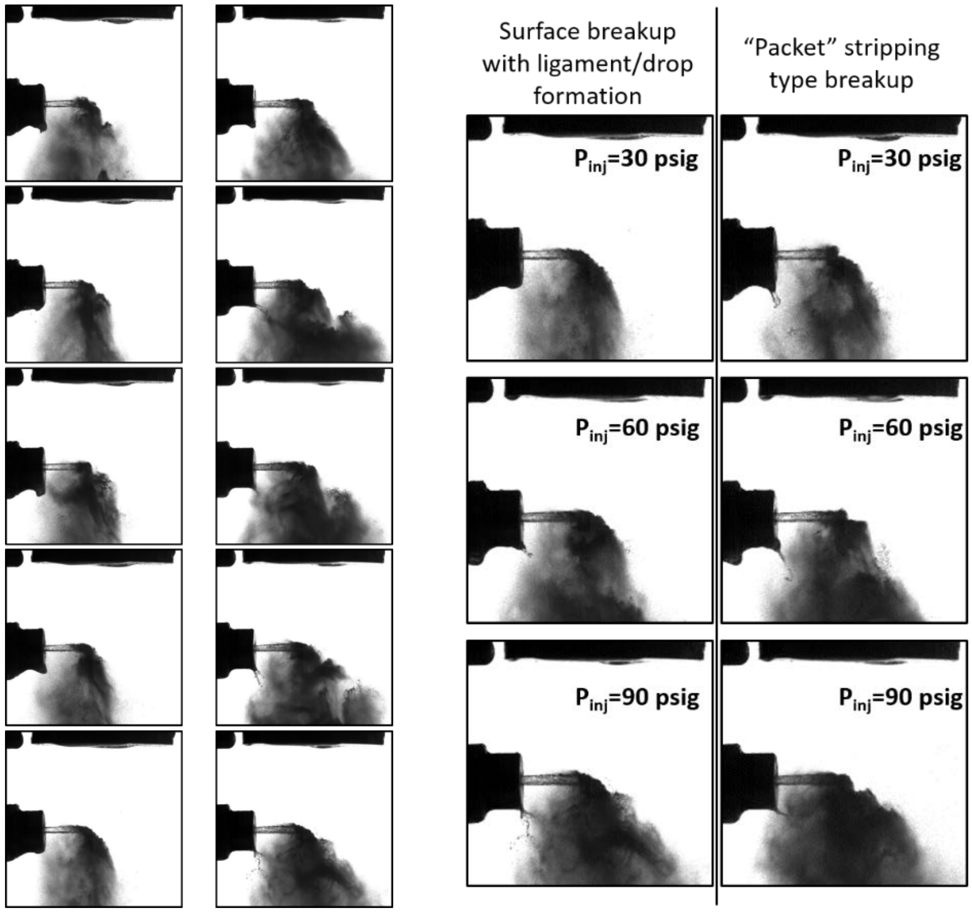

Figure 7: Instantaneous images of spray breakup for q=0.83 and q=2.5 (Left); Impact of jet momentum flux ratio on breakup process (Right). All data are for Nozzle 3.

Figure 7 shows a time sequence of images of the spray breakup for water injection using nozzle 3 for two cases of momentum flux ratio, q=0.83 and q=2.5. The time sequence is from top to bottom. The images were obtained using the diffused backlit technique utilizing the pulsed laser. The images are spaced 67 ms apart. The increase in momentum flux ratio can be observed distinctly with the images for q=2.5 showing much more penetration into and through the air jet. Regarding the breakup regime, it is clear that no column breakup similar to that illustrated in **Figure 2** (Right) is observed. The most likely explanation for this observation is that the water jet does not have significant time to be completely influenced by the crossflowing air jet. Due to the small relative size of the air jet, there is insufficient time for the generation of column waves, which grow in size and are responsible for the eventual breakup. The jet breakup and spray generation behavior seen in **Figure 7** seems to be most closely related to a surface breakup characterized by the stripping of liquid mass off the surface of the jet in the form of droplets. In all cases, the water jet is observed to remain coherent until close to the point of impact with the crossflow. However, an additional breakup behavior referred to in this work as "packet stripping" type breakup is observed in the images. This breakup behavior is associated with a complete breakdown and convection of a block of fluid in almost a vertical shearing action. Both types of breakup behavior were observed for all nozzles (Nozzles 1, 2, and 3) and momentum flux ratios.

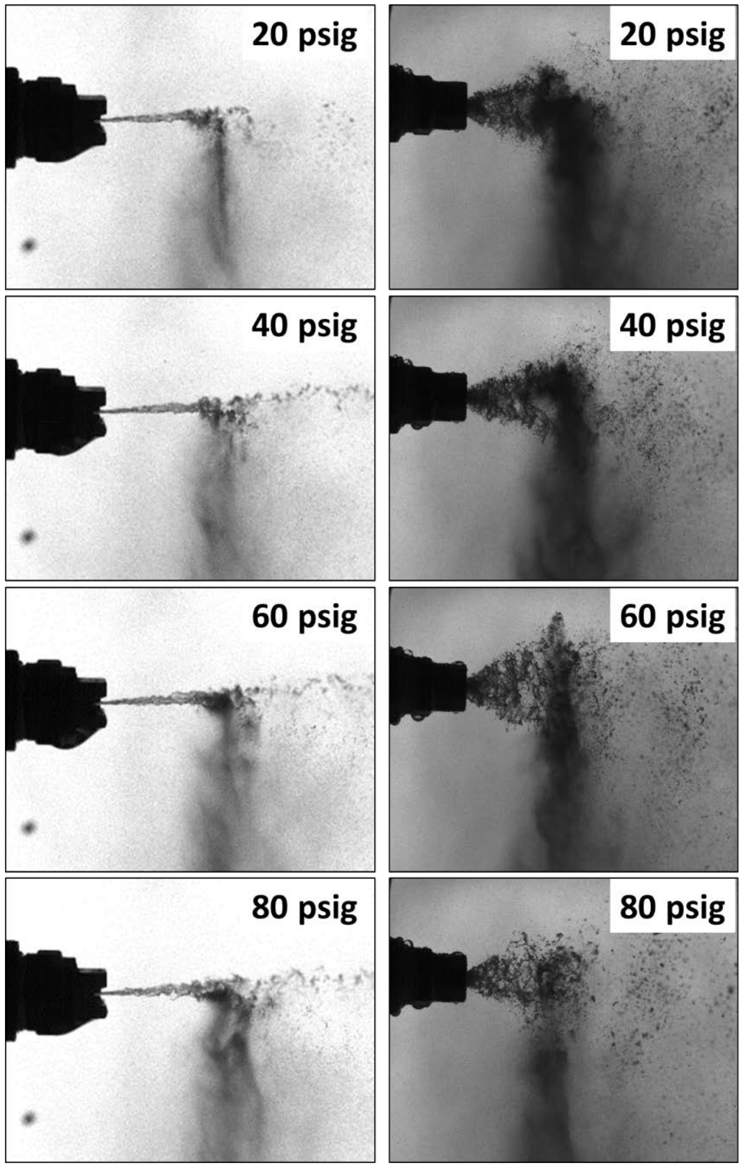

Figure 8: Instantaneous spray images from the fan-spray nozzle (left) and conical spray nozzle (right) at various injection pressures.

Figure 8 shows instantaneous images captured using diffused back-lit imaging of the fan and cone-spray nozzles producing water sprays impinging on the air jet. The test conditions correspond to different water injection pressures with total air pressure maintained at a constant value of 140 psig. Water injection pressure was varied from 20 to 80 psig. A few key distinguishing features are readily visible for the spray cases in **Figure 8** as opposed to the coherent jet breakup shown in **Figure 7**. First, for both the fan and cone sprays, the spray width at the point of intersection is larger than the width of the air jet. This results in some part of both the fan and cone sprays passing through the intersection region without direct interaction with the air jet. This can be observed in **Figure 8** as ligaments and droplets, captured by the camera, which are passing in front of the air jet. Second, both the fan and cone nozzles show distinct spray features such as ligaments and droplets prior to intersection with the air jet unlike the coherent jet cases shown in **Figure 7**. The resulting interaction for the fan and spray nozzles is more of a secondary atomization, with the portion of the spray interacting with the air jet producing a finer spray than that observed in **Figure 7** upon first impact of the air jet with the coherent water jet. Third, the secondary atomization observed in **Figure 8** appears qualitatively different, in that, the interaction process does not produce a cone-like spray as seen in **Figure 7**. Rather, the portion of the spray that interacts with the air jet appears to produce a fine spray that follows the trajectory of the air jet rather than being spread out as seen in **Figure 7**.

b. Water jet penetration

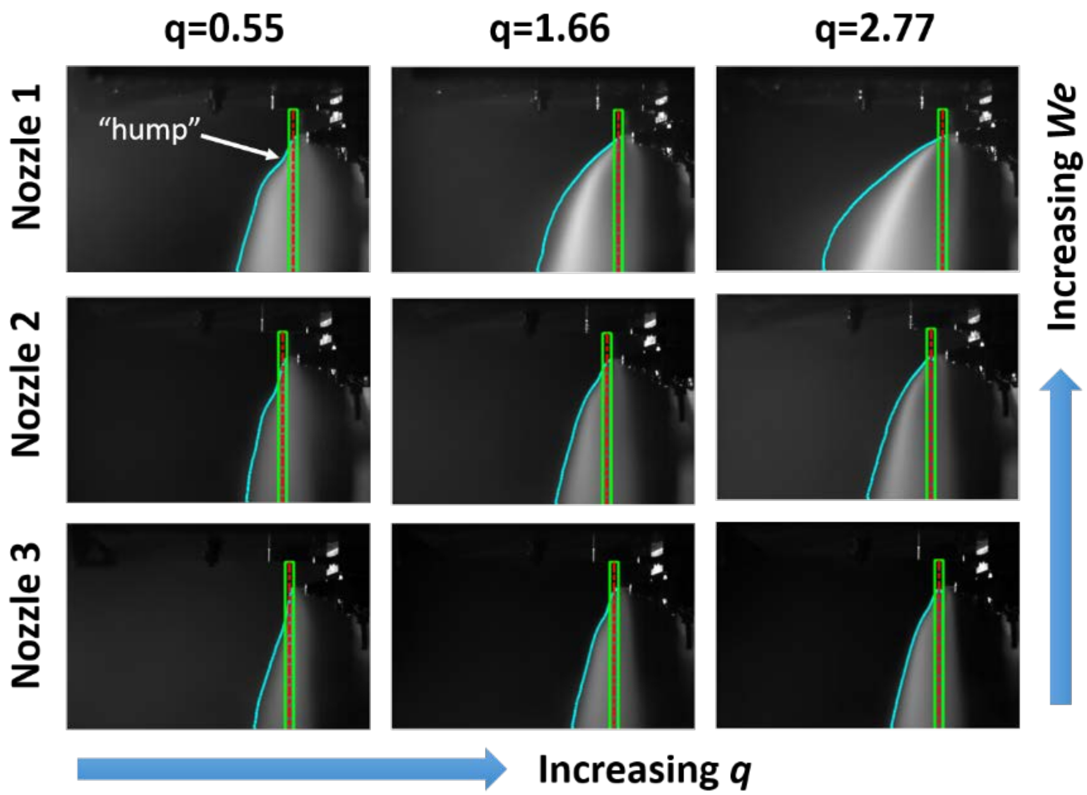

Figure 9: Effect of variation in momentum flux ratio and Weber number on water jet penetration.

Figure 9 shows results from tests conducted using the coherent jet nozzles (Nozzles 1, 2, and 3), where volume-illuminated imaging was used to obtain water spray penetration into the air jet for varying jet momentum flux ratios and Weber number. The blue lines in **Figure 9** show the edge of the water spray detected using an image processing routine where 2000 images for each case are smoothed, binarized, thresholded, and averaged in a consistent manner. The green vertical lines represent the edges of the air jet as it issues from the converging-diverging nozzle. As seen in **Figure 9**, increasing the momentum flux ratio for a fixed nozzle size results in the water jet being able to penetrate completely through the air jet. Increasing the Weber number at a fixed momentum flux ratio has a similar effect. A "hump" like feature is observed at low momentum flux ratios and low Weber numbers, where the air jet appears to have sufficiently weakened to allow the water spray the ability to push outwards. This feature is not visible at higher momentum flux ratios or higher Weber numbers.

Figure 10 shows the water jet penetration trajectory as extracted from the volume-illuminated images for the three coherent-jet nozzles, at various water injection pressures. As expected, increasing injection pressure (and hence momentum flux ratio) results in deeper penetration of the water jet into the air jet. The "hump"-like feature observed in **Figure 9**, is also visible in the jet trajectories shown in **Figure 10**.

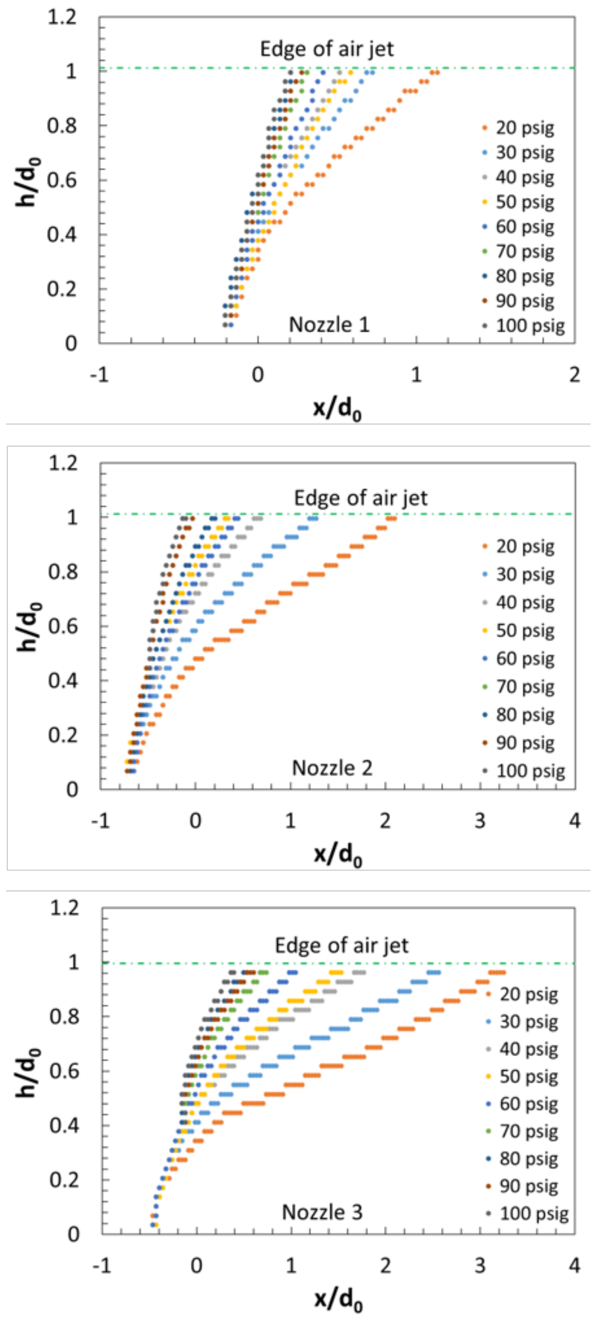

Figure 10: Water jet penetration trajectory into the air jet for three different size nozzles.

Figure 11 shows the water spray penetration trajectories for four cases of momentum flux ratio plotted for each of the three coherent jet water nozzles used in this work. The trajectories estimated using the volume-illuminated high-speed imaging results are compared with predictions from two correlations. One correlation is attributed to Yates [8] and is chosen since it is an expression used at NASA SSC to design water injection systems for rocket exhaust cooling. It is logarithmic in form and can be expressed as follows,

$$\frac{h}{d_l} = 1.1q^{0.5}ln\left(1 + 10\frac{x}{d_l}\right)$$

The other correlation is a power law form by Wu [9] and is developed for liquid jets injected into a subsonic crossflow. It is expressed as follows,

$$\frac{h}{d_l} = 4.3q^{0.33}\left(\frac{x}{d_l}\right)^{0.33}$$

As observed in **Figure 11**, the existing correlations, which were derived from experimental data do not agree well with the current measurements. This is not surprising, since the experimental configurations used to derive the correlations by Yates and Wu were primarily of the kind shown in **Figure 1** (left), with a liquid jet injected into an unbounded supersonic crossflow. An interesting point to note is the collapse of the experimental data from the different sized nozzles, onto a single curve at higher momentum flux ratios.

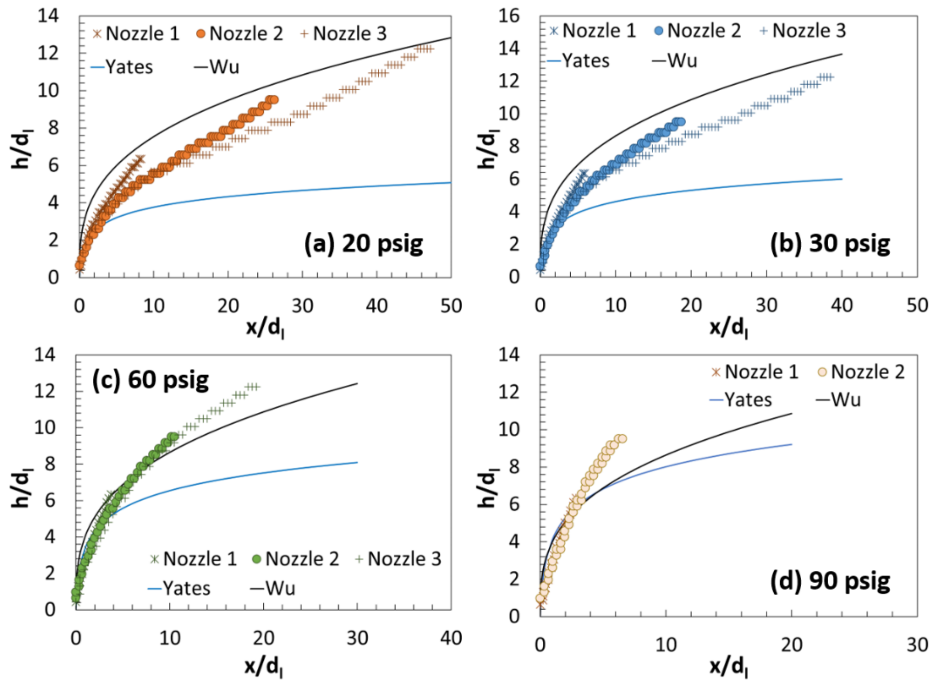

Figure 11: Comparison of spray penetration trajectory with literature correlations.

V. Conclusions

The interaction of a coherent jet or a spray with a free supersonic jet is of interest in several engineering applications. Further, it is a benchmark problem, which can be used to validate multi-phase, compressible flow codes under development at NASA SSC. To this end, an experimental investigation is undertaken in this work to characterize the interaction process using non-intrusive diagnostics. The interaction between an over-expanded supersonic free air jet with a coherent water jet results in a spray formation process that can primarily be classified as a surface breakup type phenomenon. However, a distinct "packet-stripping" type breakup is also observed. The interaction of the same air jet with a fan and full-cone type spray is distinct from that with the coherent jet. In the case of the fan and full-cone type spray, the interaction yields a finer spray that is closer to a secondary atomization process as opposed to primary atomization in the case of the coherent jet. Finally, spray penetration data measured for the water nozzles producing the coherent jets are compared with existing correlations from literature. Distinctions are noted and primarily attributed to the differences in configuration between the present case and those in previous works.

Acknowledgements

This work is supported by NASA EPSCoR and the Board of Regents of the state of Louisiana. We would like to thank Dr. Daniel Allgood from NASA Stennis Space Center for his support and collaboration.

References

[1] Krothapalli, A., Venkatakrishnan, L., Lourenco, L., Greska, B., & Elavarasan, R. (2003). Turbulence and noise suppression of a high-speed jet by water injection. Journal of Fluid Mechanics, 491, 131-159.

[2] Sachdev, J., Ahuja, V., Hosangadi, A., & Allgood, D. (2010, July). Analysis of flame deflector spray nozzles in rocket engine test stands. In 46th AIAA/ASME/SAE/ASEE Joint Propulsion Conference & Exhibit (p. 6972).

[3] Perurena, J. B., Asma, C. O., Theunissen, R., & Chazot, O. (2009). Experimental investigation of liquid jet injection into Mach 6 hypersonic crossflow. Experiments in fluids, 46(3), 403-417.

[4] Shelar, V. M., Rao, S., Hegde, G. M., Umesh, G., Jagadeesh, G., & Reddy, K. P. J. (2014). Acetone planar laser-induced fluorescence for supersonic flow visualization in air and nitrogen jet. International Journal of Mechanical and Materials Engineering, 9(1), 28.

[5] Madabhushi, R. K., Leong, M. Y., Arienti, M., Brown, C. T., & McDonell, V. G. (2006, May). On the breakup regime map of liquid jet in crossflow. In 19th Annual Conference on Liquid Atomization and Spray Systems, Toronto, Canada, May (pp. 23-26).

[6] Jones, H. (2018). Liquid Jet Penetration and Breakup in a Free Supersonic Gas Jet.

[7] Jones, H. J., Rajora, V., & Menon, S. K. (2018). Investigation of water jet break up by supersonic rocket exhaust. In 2018 International Energy Conversion Engineering Conference (p. 4697).

[8] Yates, C. (1971). Liquid injection into supersonic airstreams. In 7th Propulsion Joint Specialist Conference (p. 724).

[9] Wu, P. K., Kirkendall, K. A., Fuller, R. P., Gruber, M. R., & Nejad, A. S. (1997). Spray trajectories of liquid fuel jets in subsonic crossflows. International Journal of Fluid Mechanics Research, 24(1-3).